AIMS Materials Science, 7(1): 33–45.
DOI: 10.3934/matersci.2020.1.33
Received: 27 November 2019
Accepted: 14 January 2020
Published: 16 January 2020

http://www.aimspress.com/journal/Materials

Research article

Nanomechanical characterization of a metal matrix composite reinforced with carbon nanotubes

Mateo Duarte[1], Andrés Benítez[1], Katiuska Gómez[1], Benjamín Zuluaga D[2], Juan Meza[2], Yamile Cardona-Maya[3], Juan S. Rudas[4] and César Isaza[4,*]

[1] Facultad de Ingeniería Aeronáutica, Universidad Pontificia Bolivariana, Medellín, Colombia
[2] Design of Advanced Composites (DADCOMP), Universidad Nacional de Colombia, Facultad de Minas, Departamento de Materiales y Minerales, Cl 75 No 79A 51, 050032, Medellín, Colombia
[3] Departamento de Ciencias Básicas, Universidad Católica Luis Amigó, Medellín, Colombia
[4] Grupo GIIEN, Facultad de Ingeniería, Institución Universitaria Pascual Bravo, campus Robledo, Medellín, Colombia

* **Correspondence:** Email: c.isaza2059@pascualbravo.edu.co; Tel: +5744480520ext.1181; Fax: +5744480520.

Abstract: A new technique for the manufacture metal matrix composites has recently been developed. This technique produces a structure of a metallic matrix banded structured-layers of multiwall carbon nanotubes by a diffusive processes. To understand the increase in the volumetric mechanical properties of the composite and the dispersion of the nano-reinforcement, a nanomechanical characterization was performed by nanoindentation and atomic force microscopy. From the mechanical tests performed, a stiffness and elastic modulus maps were made near the reinforced areas, then the dispersion of the nano-reinforcements and the homogeneity of the mechanical properties were accessed. The results showed an increase in the modulus of elasticity of up to 150%; and a good dispersion of the nano-reinforcements in the reinforced zone, which demonstrates the feasibility of the alternative manufacturing process for increasing the mechanical properties of the composite.

Keywords: metal matrix composites; nano-reinforcements; mechanical properties; nanoindentation; atomic force microscopy

1. Introduction

Metal matrix composites (MMCs) have been important in the development of transport-related technologies, in particular for aerospace and ground transport [1]. The main used matrices are those based on materials with a high strength to weight ratio (S = R/W). In these matrices, a significant increase in mechanical properties has been demonstrated through the use of both micron and nano sized ceramic reinforcements such as fibers and carbon particles [2], boron [3], silicon carbide [4] and glass [5]. The technological implementation of this kind of composites leads to a decrease in the fuel consumption in transport systems and, therefore, to a decreasing of polluting emissions.

In general, the manufacturing processes of MMCs based on particulate reinforcements has some drawbacks, particularly it is quite complex to obtain a good dispersion of the reinforcement into the matrix; this problem is even more complex when carbon nanotubes (CNTs) [6] are a superior tensile strength and elastic modulus than conventional engineering materials [7]. The CNTs have many applications in industry and engineering such as: field emission probes [8], nano-devices and nano-circuits [9], SPM (scanning probe microscopy) [10], sensors [11], photonics [12], biotechnology [13], chemistry and materials science [14].

For the manufacturing of nano-reinforced metal matrix composites, several authors have used powder metallurgy [15], liquid state processes [16] and diffusive processes [17]. However, for each one of these processes, the dispersion of the CNTs into the matrix has been a challenge because they are prone to suffer agglomeration. This is due to, among other causes, the high specific surface area of the CNTs (~20 m^2/g) and to the van der Waals forces developed between the matrix and reinforcement. The agglomeration of the CNTS can cause voids and clusters that are stress raisers and, therefore the mechanical performance of the composite is compromised.

Several authors have proposed modifications to the conventional manufacturing processes to overcome some of the difficulties on the dispersion of CNTs in metal matrices. For example, Esawi et al. [18] determined the appropriate conditions to disperse the CNTs in aluminum powders and found the appropriate agitation time in the ball mill machine. In their work, they also studied the chemical transformation of the reinforcements and its mechanical damage due to the process. In another study, Esawi et al. [19] dispersed the CNTs in aluminum powders by ball mill at high energy levels; subsequently the powders were compacted between copper plates and then hot rolled. It produced a composite sheet with some alignment of the CNTs due to the deformation process, leading to an increase on some of the mechanical properties in the rolling direction.

Regarding the use of powder metallurgy for the manufacturing of magnesium matrix composite materials reinforced with CNTs, several authors have tried to integrate different techniques and they have even manufactured hybrid materials in order to increase the properties of the composite material. Li et al. [20] used the CNTs on NiO/Al_2O_3 particles mechanically mixed with Mg powder, compacted at 500 MPa and sintered at 500 °C for one hour. Finally, to enhance the hardness, the mechanical strength and elastic modulus, the composite material was extruded. Other authors [21,22], used AZ31 magnesium alloy and pure magnesium plus CNTs with the aim to study the fracture behavior and the homogenization of the reinforcement in the matrix. They found that fracture toughness increases due to the action of CNTs on AZ31 magnesium alloy, however, CTNs clusters were found and therefore an optimization of the mechanical properties was not fully obtained.

Isaza et al. [23,24] manufactured by the sandwich technique two different composites: pure aluminum and AZ31 magnesium alloy, both reinforced with MWCNTs. This technique takes

advantage of the easiness to disperse and align the CNTs into polymeric matrices to finally bring the reinforcement to the metal matrix through a sintering process [25], obtaining good dispersion and some alignment degree of the CTNs into the matrix. Moreover, no harmful interphases were detected at the interface of the reinforcement and the metallic matrix allowing suitable load transfer between them. However, Zhou et al. [26], synthetized Mg–CNTs composites by powder metallurgy and different types of aluminum carbides were formed at the interface, this finding decreases some mechanical properties of the composite. Several of those studies have shown that poor dispersion of nano-reinforcements produces negative effects on the mechanical response of the composite material [27,28].

Another important aspect is the interface between the metallic matrix and the reinforcement. Several authors have studied the interface in order to understand the mechanisms of load transfer between the reinforcement and the metallic matrix. For such nano-mechanical characterization, different techniques have been used, to mention some of them: Nanoindentation [29], micro and nano-cantilever compression and flexion tests [30], nano-tension tests [31], in-situ HRTEM [32], FESEM [32] and atomic force microscopy (AFM) [33]. AFM based Nanomechanical modes, such as force modulation [34], force volume [35], lateral force microscopy [36], peak force tapping [32] and tapping mode phase imaging [37], provide sample's mechanical properties and surface topography. The AFM force-distance (FD) spectroscopy acquires the tip applied force and its position in three axis, it enables based on the force and tip vertical displacement to obtain some mechanical properties such as hardness, elastic modulus, etc. and, for this to be possible an appropriate contact mechanics model must be used [38].

Zhou et al. [39] studied the shear strength between metallic matrix and CNTs by an in-situ pull-out technique. The MWCNT was pulled out from the Al matrix using a three-axis nano-manipulator system installed inside an SEM chamber. The effective embedded length and diameter of the MWCNTs incorporated in the Al matrix were evaluated by observing the pulled out MWCNTs under HRTEM. The mechanical properties of the MWCNT/Al composites were in good agreement with the estimated load transference efficiency of 60%. Other authors studied the interfacial interactions between carbon nanotubes and aluminum and titanium matrixes [40,41], the nano-mechanical measurements revealed a shear lag effect on the CNTs-Ti interface obtaining an interfacial shear strength 32% higher compared to CNT–Al interface.

A recent AFM study performed by Zhang et al. [42] shows the capabilities of the AFM technique to explore the mechanical behavior of nano-composites. They studied the elastic modulus variation in a polylactic acid/polyε-caprolactone reinforced with CNTs nano-composite. The authors found that MWCNTs are mainly dispersed in the polyε-caprolactone phase which is adjacent to the Polylactic acid phase. The elastic modulus distribution significantly changes with the introduction of MWCNTs. No intermediate layers in the interfaces were observed, indicating weak interactions in the polymer/MWCNTs interface. The same was concluded by Zhu et al. [43], they found a poor miscibility between polyε-caprolactone and cellulose acetate butyrate by AFM tapping mode.

This work presents a microstructural and nano-mechanical characterization of composites synthetized by the sandwich technique made of AZ31 magnesium alloy and carbon nanotubes. A quantification of the dispersion of the CNTs is performed by statistical methods. A nanomechanical mapping characterization using AFM and nanoindentation was done in order to characterize the hardness and elastic modulus in the reinforced zone.

2. Materials and methods

2.1. Composites synthesis

MWCNTs were supplied by Nanostructured & Amorphous Materials Inc. (98% of purity), which have outer diameters ranging from 10 to 40 nm, inner diameters between 10 and 20 nm and lengths between 30 and 50 μm.

The composites were manufactured in two steps: initially multi-walled nanotubes (MWCNTs) were dispersed into polyvinyl alcohol (PVA) in three different weight percentages (0.25, 0.5 and 1 wt%) and mechanically aligned by stretching [25]. Then the stretched sheets of each PVA/MWCNTs percentage were stacked with sheets of the AZ31B magnesium alloy and hot compacted in a controlled atmosphere furnace. Thus, three composites were manufactured with different percentages of MWCNTs added into metal matrix. For more details of the manufacturing process, see reference [24].

2.2. Microstructural characterization

For microstructural characterization, the samples were cut and subsequently metallographically polished. The microstructure observation was performed through a field emission scanning electron microscope (FESEM) JEOL JSM-6701F. For metal matrix composites dispersion quantification, representative images were divided into 10 × 10 grid lines along the horizontal and vertical directions, then the spacing, both horizontal and vertical, between nearest MWCNTs were measured at each grid intersection using a free software Gwyddion. These data were analyzed using the statistical distribution model [25] shown below in Eq 1.

$$f(x) = \frac{1}{xn\sqrt{2\pi}} exp\left[-\frac{1}{2}\left(\frac{lnx-m}{n}\right)^2\right] \; for \; x > 0$$
$$f(x) = 0 \; for \; x \leq 0 \tag{1}$$

where $m = ln\frac{u^2}{\sqrt{u^2+\sigma^2}}$ and $n = \sqrt{ln\frac{u^2+\sigma^2}{u^2}}$, x is the free-path distance, u is the mean and σ is the standard deviation for the free-path distance measured.

2.3. Atomic force microscope characterization

The composites samples were characterized by AFM in order to evidence the homogenous dispersion of the MWCNTs into metal matrix. The tests were performed on a Park Systems® device (Park NX10) and the PinPoint mode was used with a CONTSCR micro-cantilever using a constant load of 20 nN. The pin point mode allows to obtain sample's stiffness mapping through force-distance (F-D) acquired at each pixel over the entire scan area. In this mode, the surface morphology as well as the quantitative nanomechanical properties (i.e., modulus, adhesion, deformation and dissipation) of the sample can be obtained, in other words this mode could allow detecting phase changes. An Approach time of 3.0 ms, retract time of 2.0 ms, stiffness threshold of 8.00 nN and FMR probe by Park System with force constant of 2.8 N/m and resonance frequency

of 75 kHz were used as instrument setup. The spring constant and sensitivity calibration was conducted on a bare Si wafer before to start the measurements. There, the deflection was converted to a force using the spring constant of the cantilever (2.003 N/m). A tip sensitivity of 29.18 V/μm was obtained. The AFM scanning were carried out in an area of 5 μm × 5 μm in the reinforced zone and the results will show the contrast mapping for elastic modulus in the interface between magnesium layers; however, this result only allows a qualitative relationship between the composites studied. Therefore, this map allows a direct comparison with the MWCNTs dispersion results obtained by FESEM images and nanoindentation test as will be seen later.

2.4. Nanoindentation characterization

The nanoindentation tests were performed on an IBIS Authority Fischer-Cripps with a Berkovich-type diamond tip in closed loop mode. It was scanned an area of 50 μm × 25 μm with a maximum load of 1 mN producing a maximum depth of about 200 nm. Then, to obtain more detailed information, it was scanned an area of 5 μm × 5 μm with a maximum load of 0.3 mN producing a maximum depth of about 50 nm. For both tests, the separation between indentations were more than 5 times the maximum penetration in order to avoid the effect from surrounding indentations as demonstrated Cheng et al. [44,45] (separations of 5 μm and 250 nm for maximum loads of 1 mN and 0.3 mN, respectively). The mechanical properties were deconvoluted using the Oliver and Pharr method [44,45] and then plotted in contour curves shown in Figures 4 to 6.

3. Results and discussions

3.1. Microstructural characterization

Microstructures for each of the manufactured composites are shown in Figure 1. In the reinforced zones (study zone or diffusion zone, that corresponds to the interface between the magnesium sheets where the PVA sheet reinforced with MWCNTs were placed), MWCNTs are embedded in the magnesium matrix as is shown in Figure 1b–d for the magnesium reinforced with 0.25, 0.5 and 1.0 wt% of MWCNTs, respectively. Figure 1a shows the microstructure of the material manufactured without reinforcement, that is, the material compacted by the sandwich technique and, the diffusion area between the magnesium sheets is evidenced.

In the microstructures analyzed, it can be seen that the MWCNTs are well dispersed in the magnesium matrix. In addition, as seen in Figures 1a–d, pores due to the manufacturing process are not evidenced. Therefore, an increasing in the mechanical properties at a volumetric level is expected [24].

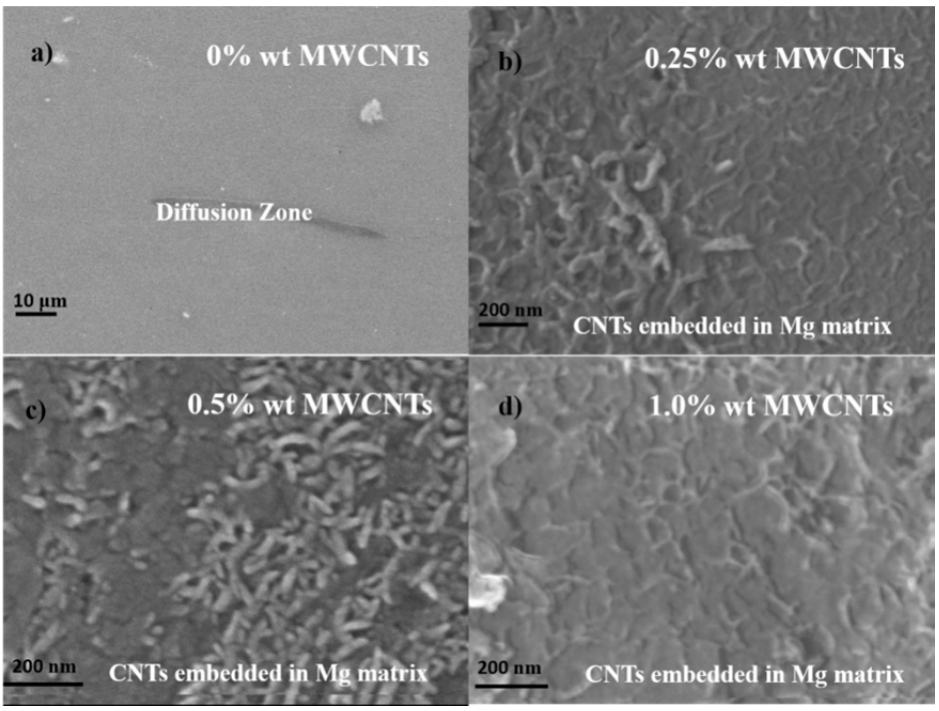

Figure 1. FESEM micrographs. (a) 0 wt% MWCNTs, (b) 0.25 wt% MWCNTs, (c) 0.5 wt% MWCNTs, and (d) 1.0 wt% MWCNTs.

3.2. Quantification of the CNTs dispersion

For the dispersion quantification, the methodology described above (section 2.2) was used. The data obtained from the measurements of the horizontal and vertical distances were plotted below the micrographs as a histogram, which shows a lognormal distribution as seen in Figure 2a–c for each of the manufactured composites. From the histograms, the degree of dispersion was calculated following the procedure proposed in reference [25].

Figure 2a shows for the composite material reinforced with 0.25 wt% of MWCNTs an average distance between MWCNTs of 33.1 nm with a standard deviation of 19.25 nm. For this composite, most of the data is in the range of 20–28 nm. Similarly, Figure 2b shows for the composite reinforced with 0.5 wt% of MWCNTs, an average distance between MWCNTs of 22.2 nm with a standard deviation of 23.4 nm, most of the data is in the range of 15–20 nm. Finally, for the composite reinforced with 1.0 wt% of MWCNTs (Figure 2c) reveals an average distance between MWCNTs of 30.6 nm with a standard deviation of 29.8 nm, and most of the data is in the range of 20–30 nm. It is important to mention that the differences in the image sharpness is due to the difference in the CNTs depths respect to the surface level, in other words in some cases as Figure 2b CNTs are completely exposed, while in the other cases they are beneath the surface covered by magnesium.

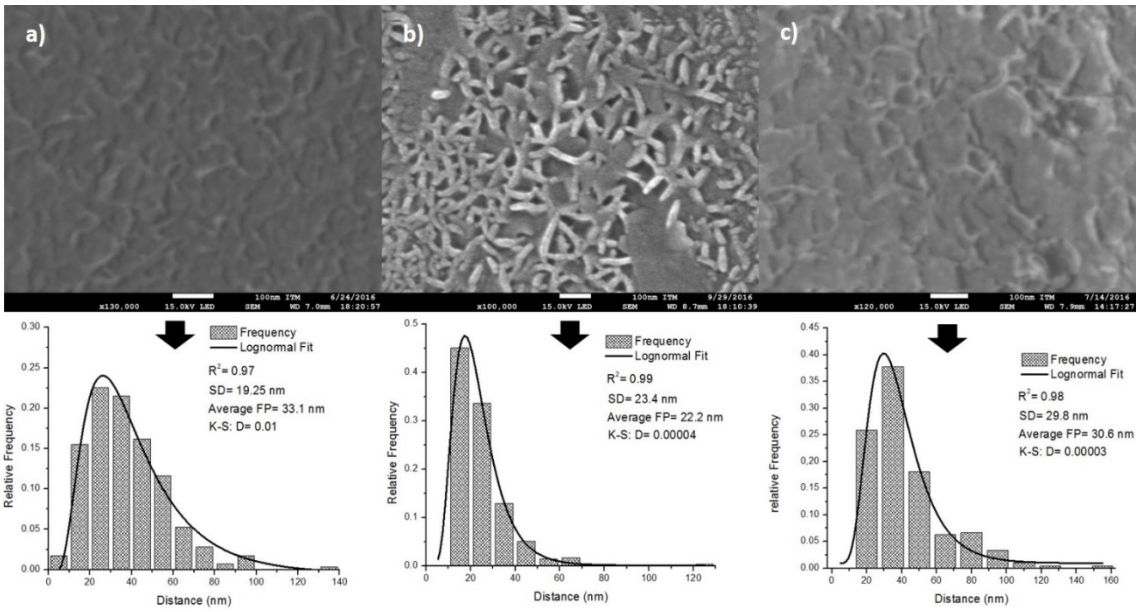

Figure 2. CNTs dispersion: (a) 0.25% CNTs, (b) 0.5% CNTs, and (c) 1.0% CNTs.

The results show that the dispersion of MWCNTs has a similar behavior, i.e., their average separations with the addition of MWCNTs in metal matrix are similar; this can be due to the sonication energy ranges used. The quantification of the dispersion degree, which measures the percentage of MWCNTs that are in a separation range (most of data that are within the range), reveals values between 8.39 and 14.40%, much better values compared to other studies that reached values of only 4% [46].

However, this quantification may vary between study areas for the same composites, among other reasons, due to heterogeneities in the diffusive process. Clearly, there is a high standard deviation, which is lower for low MWCNTs contents, which also means a better and more homogeneous dispersion of the reinforcement. Therefore, a more detailed study of this parameter is required for future research. In Table 1 is summarized the data obtained. This data can be compared with the data reported in [25] for the polymer matrix composites reinforced with MWCNTs, however, during the hot compacted process, diffusion occurs and the MWCNTs distances can be change.

Table 1. Measured and calculated parameters for the Mg–MWCNTs composites.

Sample (wt% MWCNTs)	Average free path (nm)	Standards deviation (nm)	$D_{0.1}$
Mg-0.25 wt%	33.1	19.25	14.40
Mg-0.5 wt%	22.2	23.4	8.39
Mg-1.0 wt%	30.6	29.8	9.01

3.3. AFM results

Figure 3 shows the results of the AFM pin point tests, which were analyzed with the Gwddion software in its free version. The images show a mapping of the stiffness, bright colored zones correspond to bigger stiffness. It must be kept in mind the measured stiffness is not accurate, because it highly depends on: the cantilever tip roundness and on the choice of the region of the

force-distance curve; we fixed these conditions so the bias is always the same extent for all the samples. Moreover, the reported stiffness is influenced by the surroundings, included those beneath the sampled surface, in other words the sampled zone can be thought as a system of parallel springs where each phase has its own stiffness (like in a coated system). This can partially explain the differences in the maximum values of the stiffer regions. This effect is minimized when the penetration depth of the cantilever tip is increased as in the case of any indentation test: at higher loads a mean effect of all the phases indented is sensed. Some profiles were also made, it is evident that there is a dispersion of the areas with bigger stiffness; it suggests MWCNTs dispersion in the matrix was appropriated allowing to obtain very good mechanical properties as shown in this research.

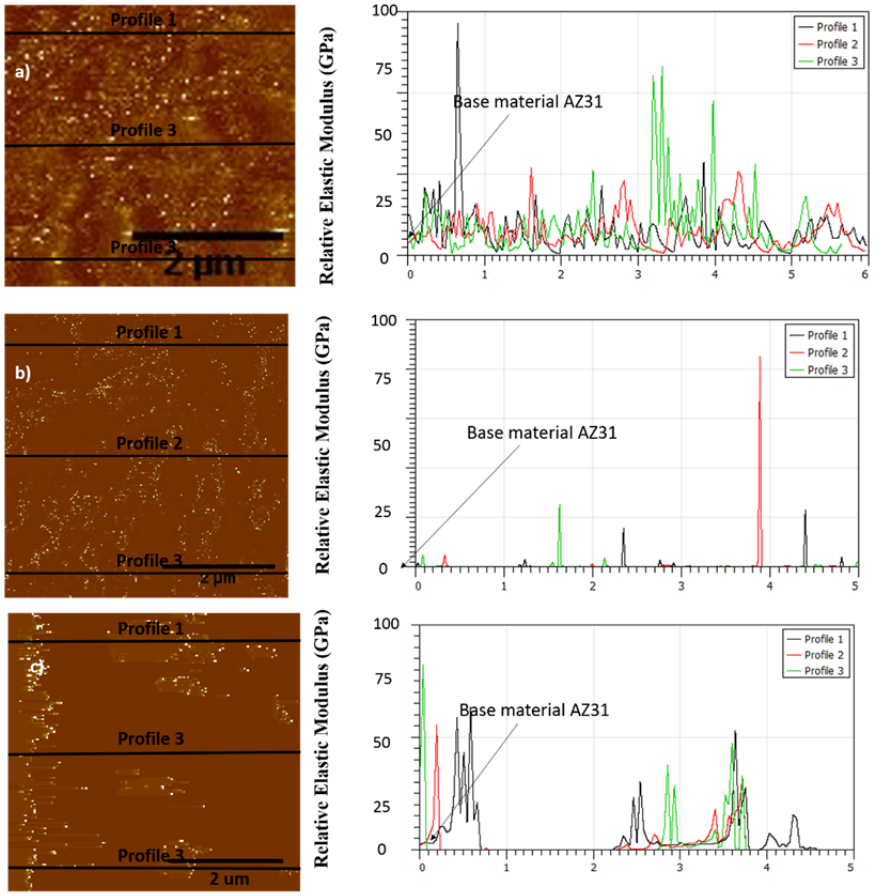

Figure 3. PinPoint AFM mode at the interface between magnesium sheets. (a) 0.25 wt%, (b) 0.5 wt%, and (c) 1.0 wt% of MWCNTs. Bright colored zones correspond to bigger sample stiffness.

3.4. Nanoindentation results

For the nanoindentation tests, two modulus mappings were performed as described in section 2.4. The first mapping was carried out in an area that evidenced the change between the base material (sheets of Mg alloy) and the reinforced area (Mg plus CNTs or "diffusion zone"). The second mapping, which is a close up of the initial mapping, was performed in the reinforced area with an

increase in the resolution in the measuring of the mechanical properties.

Figure 4 shows the mapping (Figure 4a) and a detail mapping (Figure 4b) of the reinforced area for the composite manufactured with 0.25 wt% of MWCNTs, besides the Figure 4c shows the representative nanoindentation data curves for the maximum loads used (0.3 and 1 mN). Figure 4a shows that the elastic modulus goes from 45 GPa for the base material up-to about 120 GPa in the reinforced zone. In addition, in the reinforced zone shown in Figure 4b, it can be seen that the reinforcing phase (that has an elastic modulus greater than the matrix) is properly dispersed. As has been seen above, this has been validated by the microstructural characterization and by qualitative AFM mapping.

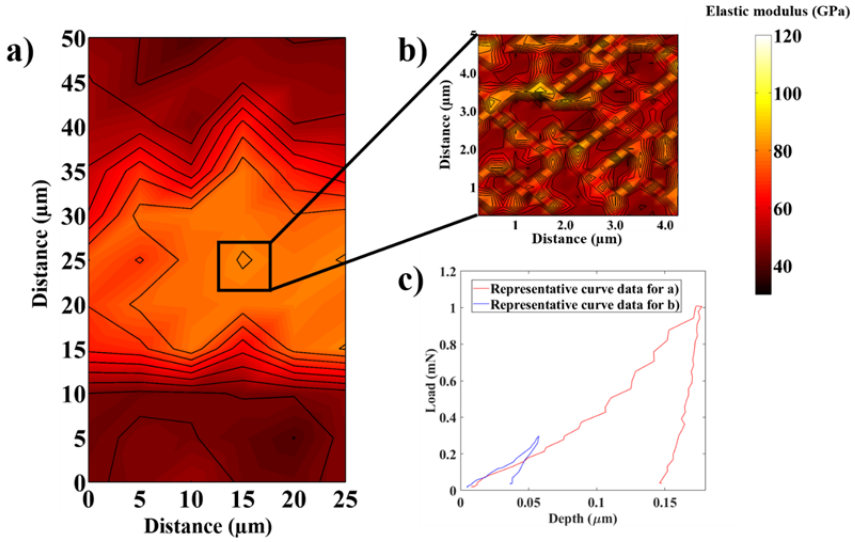

Figure 4. Nanoindentation data for composite reinforced with 0.25 wt% added into metallic matrix. (a) Nanoindentation mapping in a scanned area of 50 μm × 25 μm and a maxima load of 1 mN, (b) detailed nanoindentation mapping in a scanned area of 5 μm × 5 μm and a maximum load of 0.3 mN, and (c) Representative data curve for both (loads of 0.3 and 1 mN).

Finally, for composites manufactured with 0.5 and 1 wt% of MWCNTs, Figures 5 and 6 shown a similar trend to the 0.25 wt% of MWCNTs composite, i.e, the elastic modulus change from 45 GPa up-to about 100 and 120 GPa, respectively (Results obtained for nanoindentation load of 1mN). In addition, for these two composites, there is a decrease in the dispersion of the reinforcing phase, but a greater elastic modulus with respect to the composite manufactured with 0.25 wt% of MWCNTs was evidenced (Results obtained for nanoindentation load of 0.3 mN). This is consistent with what was observed through AFM and FESEM analysis; in other words, MWCNTs are closer and are present in more quantity for the composites reinforced with 0.5 and 1 wt% of MWCNTs. It is important to clarify that the elastic modulus of the MWCNTs are about 800–1000 GPa, while the data obtained in the composites even when the indenter tip is placed on top of a CNT are influenced by penetration depth of the indenter tip, i.e., by the volume of the sampled zone. A very shallow indentation (on the order of 2–5 nm) is required to obtain values closer to the CNTs.

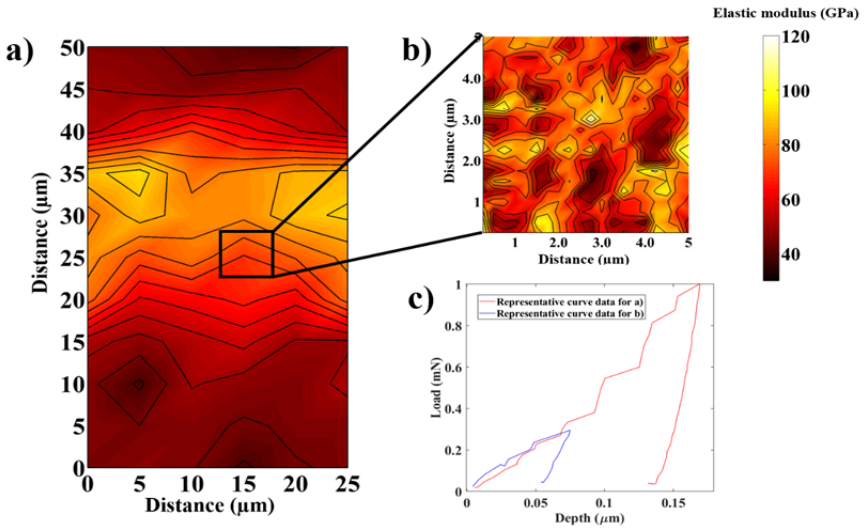

Figure 5. Nanoindentation data for composite reinforced with 0.5 wt% added into metallic matrix. (a) Nanoindentation mapping in a scanned area of 50 μm × 25 μm and a maxima load of 1 mN, (b) detail nanoindentation mapping in a scanned area of 5 μm × 5 μm and a maxima load of 0.3 mN, and (c) Representative data curve for both (loads of 0.3 and 1 mN).

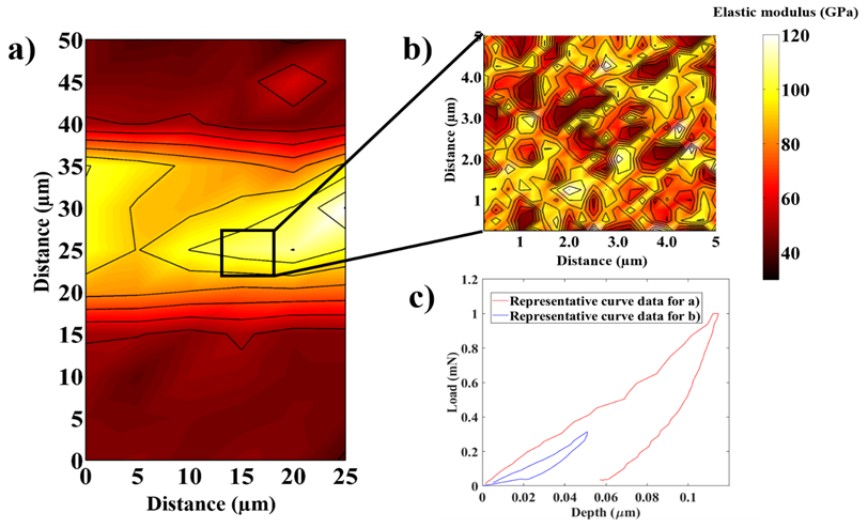

Figure 6. Nanoindentation data for composite reinforced with 1.0 wt% added into metallic matrix. (a) Nanoindentation mapping in a scanned area of 50–25 μm and a maxima load of 1 mN, (b) detail nanoindentation mapping in a scanned area of 5 μm × 5 μm and a maxima load of 0.3 mN, and (c) Representative data curve for both (loads of 0.3 and 1 mN).

4. Conclusions

With the characterization techniques used in this study, it was possible to demonstrate the increase of the mechanical properties in the reinforced zones by the action of reinforcement, this

characterization validate the increase of mechanical properties in bulk shown in previous works. In addition, it was possible to demonstrate a well dispersed MWCNTS in metal matrix by FESEM, AFM and nanoindentation test. Although the ideal situation is to have a 100%-degree dispersion (all reinforcements are the same distance), reaching a 10%-degree dispersion is promising compared to other studies that show 3% and 4% dispersion degrees. This dispersion is reflected in the increase of the mechanical properties at volumetric and micrometric level (as demonstrated by the qualitative stiffness mapping through AFM and the quantitative elastic modulus mapping by nanoindentation test).

Finally, the increase in the elastic modulus in the study area respect to the magnesium were: 100%, 110% and 130% for composites manufactured with 0.25, 0.5 and 1 wt% of MWCNTs added into magnesium matrix. These increases are significant and evidence the appropriate dispersion of the reinforcement achieved in the reinforced zone.

Acknowledgments

We would like to thank at Institución Universitaria Pascual Bravo for the financial support with the research "Desarrollo de materiales metálicos livianos nano-reforzados por medio de técnicas alternativas" and to the Universidad Nacional of Colombia, sede Medellín, for allowing the use of the LTDM laboratory.

Conflict of interests

The authors declare no conflicts of interest.

References

1. González C, Vilatela J, Molina-Aldareguia J, et al. (2017) Structural composites for multifunctional applications: current challenges and future trends. *Prog Mater Sci* 89: 194–251.
2. Parizi MT, Ebrahimi G, Ezatpour H, et al. (2019) The structure effect of carbonaceous reinforcement on the microstructural characterization and mechanical behavior of AZ80 magnesium alloy. *J Alloy Compd* 809: 151682.
3. Lakshmanan P, Dharmaselvan S, Paramasivam S, et al. (2019) Tribological properties of B_4C nano particulates reinforced copper matrix nanocomposites. *Mater Today Proc*16: 584–591.
4. Poletti C, Balog M, Schubert T, et al. (2008) Production of titanium matrix composites reinforced with SiC particles. *Compos Sci Technol* 68: 2171–2177.
5. Reddy B, Narayana KB (2018) Fabrication, testing and evaluation of mechanical properties of woven glass fibre composite material. *Mater Today Proc* 5: 2429–2434.
6. Song YS, Youn JR (2005) Influence of dispersion states of carbon nanotubes on physical properties of epoxy nanocomposites. *Carbon* 43: 1378–1385.
7. Lanfant B, Leconte Y, Debski N, et al. (2019) Mechanical, thermal and electrical properties of nanostructured CNTs/SiC composites. *Ceram Int* 45: 2566–2575.
8. Jayakumar J, Raghunath BK, Rao TH (2013) Enhancing microstructure and mechanical properties of AZ31–MWCNT nanocomposites through mechanical alloying. *Adv Mater Sci Eng* 2013: 1–6.

9. Cottet A, Dartiailh MC, Desjardins MM, et al. (2017) Cavity QED with hybrid nanocircuits: from atomic-like physics to condensed matter phenomena. *J Phys-Condens Mat* 29: 433002.
10. Mukhin I, Fadeev I, Zhukov M, et al. (2015) Framed carbon nanostructures: synthesis and applications in functional SPM tips. *Ultramicroscopy* 148: 151–157.
11. Zhao Q, Gan Z, Zhuang Q (2002) Electrochemical sensors based on carbon nanotubes. *Electroanalysis* 14: 1609–1613.
12. Avouris P, Freitag M, Perebeinos V (2008) Carbon-nanotube photonics and optoelectronics, Nature photonics. *Nat Photonics* 2: 341–350.
13. Bekyarova E, Ni Y, Malarkey EB, et al. (2005) Applications of carbon nanotubes in biotechnology and biomedicine. *J Biomed Nanotechnol* 1: 3–17.
14. Zhang Z, Zhang Y, Jiang X, et al. (2019) Simple and efficient pressure sensor based on PDMS wrapped CNT arrays. *Carbon* 155: 71–76.
15. Munir KS, Kingshott P, Wen C (2015) Carbon nanotube reinforced titanium metal matrix composites prepared by powder metallurgy—a review. *Crit Rev Solid State* 40: 38–55.
16. Sahoo BP, Das D (2019) Critical review on liquid state processing of aluminium based metal matrix nano-composites. *Mater Today Proc* 19: 493–500.
17. Ren H, Ren X, Xiong H, et al. (2019) Nano-diffusion bonding of Ti2AlNb to Ni-based superalloy. *Mater Charact* 155: 109813.
18. Esawi AM, Morsi K, Sayed A, et al. (2009) Fabrication and properties of dispersed carbon nanotube–aluminum composites. *Mater Sci Eng A-Struct* 508: 167–173.
19. Esawi AM, El Borady MA (2008) Carbon nanotube-reinforced aluminium strips. *Compos Sci Technol* 68: 486–492.
20. Li H, Fan J, Geng X, et al. (2014) Alumina powder assisted carbon nanotubes reinforced Mg matrix composites. *Mater Design* 60: 637–642.
21. Sun F, Shi C, Rhee KY, et al. (2013) In situ synthesis of CNTs in Mg powder at low temperature for fabricating reinforced Mg composites. *J Alloy Compd* 551: 496–501.
22. Jayaraman J, Kuppusamy R, Rao H (2016) Investigation on wear properties of AZ31-MWCNT nanocomposites fabricated through mechanical alloying and powder metallurgy. *Sci Eng Compos Mater* 23: 61–66.
23. Isaza MCA, Ledezma Sillas JE, Meza JM, et al. (2017) Mechanical properties and interfacial phenomena in aluminum reinforced with carbon nanotubes manufactured by the sandwich technique. *J Compos Mater* 51: 1619–1629.
24. Merino CAI, Sillas JL, Meza J, et al. (2017) Metal matrix composites reinforced with carbon nanotubes by an alternative technique. *J Alloy Compd* 707: 257–263.
25. Isaza MCA, Herrera Ramirez JM, Ledezma Sillas JE, et al. (2018) Dispersion and alignment quantification of carbon nanotubes in a polyvinyl alcohol matrix. *J Compos Mater* 52: 1617–1626.
26. Zhou W, Bang S, Kurita H, et al. (2016) Interface and interfacial reactions in multi-walled carbon nanotube-reinforced aluminum matrix composites. *Carbon* 96: 919–928.
27. Ghasemi A, Penther D, Kamrani S (2018) Microstructure and nanoindentation analysis of Mg-SiC nanocomposite powders synthesized by mechanical milling. *Mater Charact* 142: 137–143.
28. Salama EI, Abbas A, Esawi AM (2017) Preparation and properties of dual-matrix carbon nanotube-reinforced aluminum composites. *Composites Part A-Appl S* 99: 84–93.

29. Maja ME, Falodun OE, Obadele BA, et al. (2018) Nanoindentation studies on TiN nanoceramic reinforced Ti–6Al–4V matrix composite. *Ceram Int* 44: 4419–4425.
30. Pingkarawat K, Mouritz A (2016) Comparative study of metal and composite z-pins for delamination fracture and fatigue strengthening of composites. *Eng Fract Mech* 154: 180–190.
31. Ruoff RS, Qian D, Liu WK (2003) Mechanical properties of carbon nanotubes: theoretical predictions and experimental measurements. *Cr Phys* 4: 993–1008.
32. Wang D, Russell TP, Nishi T, et al. (2013) Atomic force microscopy nanomechanics visualizes molecular diffusion and microstructure at an interface. *ACS Macro Lett* 2: 757–760.
33. Xavior MA, Kumar HP (2017) Processing and characterization techniques of graphene reinforced metal matrix composites (GRMMC); a review. *Mater Today Proc* 4: 3334–3341.
34. Radmacher M, Tillmann R, Gaub H (1993) Imaging viscoelasticity by force modulation with the atomic force microscope. *Biophys J* 64: 735–742.
35. Wang D, Fujinami S, Nakajima K, et al. (2010) True surface topography and nanomechanical mapping measurements on block copolymers with atomic force microscopy. *Macromolecules* 43: 3169–3172.
36. Tocha E, Schönherr H, Vancso GJ (2006) Quantitative nanotribology by AFM: a novel universal calibration platform. *Langmuir* 22: 2340–2350.
37. Scott WW, Bhushan B (2003) Use of phase imaging in atomic force microscopy for measurement of viscoelastic contrast in polymer nanocomposites and molecularly thick lubricant films. *Ultramicroscopy* 97: 151–169.
38. Wang D, Russell TP (2017) Advances in atomic force microscopy for probing polymer structure and properties. *Macromolecules* 51: 3–24.
39. Zhou W, Yamamoto G, Fan Y, et al. (2016) In-situ characterization of interfacial shear strength in multi-walled carbon nanotube reinforced aluminum matrix composites. *Carbon* 106: 37–47.
40. Yi C, Chen X, Gou F, et al. (2017) Direct measurements of the mechanical strength of carbon nanotube-aluminum interfaces. *Carbon* 125: 93–102.
41. Yi C, Bagchi S, Dmuchowski CM, et al. (2018) Direct nanomechanical characterization of carbon nanotubes-titanium interfaces. *Carbon* 132: 548–555.
42. Zhang S, Liu H, Gou J, et al. (2019) Quantitative nanomechanical mapping on poly(lactic acid)/poly(-caprolactone)/carbon nanotubes bionanocomposites using atomic force microscopy. *Polym Test* 77: 105904.
43. Zhu B, Wang X, Zeng Q, et al. (2019) Enhanced mechanical properties of biodegradable poly (-caprolactone)/cellulose acetate butyrate nanocomposites filled with organoclay. *Compos Commun* 13: 70–74.
44. Chen J, Bull S (2006) On the relationship between plastic zone radius and maximum depth during nanoindentation. *Surf Coat Tech* 201: 4289–4293.
45. Chen J (2012) Indentation-based methods to assess fracture toughness for thin coatings. *J Phys D-Appl Phys* 45: 203001.
46. Luo Z, Koo JH (2007) Quantifying the dispersion of mixture microstructures. *J Microsc* 225: 118–125.